Available online at www.sciencedirect.com

ScienceDirect

Ceramics International 39 (2013) 8847–8852

CERAMICS INTERNATIONAL

www.elsevier.com/locate/ceramint

In-situ grown hydroxyapatite whiskers reinforced porous HA bioceramic

Zhou Fang[a], Qingling Feng[b,*], Rongwei Tan[c]

[a]State Key Laboratory of New Ceramics and Fine Processing, School of Materials Science and Engineering, Tsinghua University, Beijing 100084, China
[b]Key Laboratory of Advanced Materials (MOE), School of Materials Science and Engineering, Tsinghua University, Beijing 100084, China
[c]Key Laboratory of Biomedical Materials and Implants, Research Institute of Tsinghua University in Shenzhen, Shenzhen 518057, China

Received 11 March 2013; received in revised form 11 April 2013; accepted 22 April 2013
Available online 9 May 2013

Abstract

To improve the mechanical properties of a porous bioceramic without reducing its porosity, a new kind of porous hydroxyapatite (HA) bioceramic with in-situ grown HA whiskers was fabricated using a simple sintering method. $CaSO_4 \cdot 2H_2O$ was used as a pore-forming medium and also as a catalyst for the growth of in-situ HA whiskers. The bioceramic was analyzed by XRD, SEM and mechanical tests. In-situ grown HA whiskers were stratified on the cliffs of pores in the bioceramic. The compressive strength is as high as 21.7 MPa with the porosity of about 26%. The results show that porous HA bioceramic can be improved in both compressive strength and porosity by the addition of $CaSO_4 \cdot 2H_2O$. This novel HA bioceramic has a higher compressive strength without reducing its porosity in a certain weight ratio of $CaSO_4 \cdot 2H_2O$, which depends on its two-step fracture pattern. This novel structure provides a new and promising reinforced pattern for porous materials.

Keywords: C. Mechanical properties; Hydroxyapatite whiskers; Porous bioceramic

1. Introduction

Hydroxyapatite ($Ca_{10}(PO_4)_6(OH)_2$) (HA) is the major inorganic component of bones and teeth. It is widely used as restorative materials in dentistry and biomedical substitutions. HA has no toxicity but has a high biocompatibility and a perfect osteoconductivity. However, compared to human bone, the fracture toughness of pure HA is low [1], which limits its application. Porous HA scaffold is beneficial to cell growth, but its compressive strength is relatively low, ranging from 1.2 to 16 MPa, for example, a compressive strength of 4.2 MPa with a porosity of 65% [2]. In consideration of the weak mechanical properties of porous HA bioceramic, different morphologies were obtained to improve its mechanical properties. So the preparation of well-defined HA crystals with controlled morphology has been the focus of intensive research in the previous decades [3].

Previous results showed that, when introducing HA with different morphologies into the polyanhydride matrix, the improvement of mechanical properties is maximal for whisker, next for sphere, rod and flake [4]. The improvement in fracture toughness by HA whisker is mainly based on the crack bridging and crack deflection, which absorb the energy of crack propagation and eliminate stress concentration at the crack tip [5]. Recent research focused on adding whiskers to toughen HA matrixes [6] or compositing high aspect ratio HA whiskers with polymers to improve the mechanical properties of the composites [7,8]. Thus plenty methods of synthesizing HA whiskers were developed, such as high-temperature solid state reaction [9], molten salt synthesis [10] and hydrothermal treatment [11,12]. However, mechanical properties such as compressive strength of the HA/polymer composites usually decreased with the increase in HA whisker content [6,13].

Pores are necessary for bone tissue formation for the permission of migration and proliferation of osteoblasts and mesenchymal cells, as well as vascularization. Moreover, the mechanical interlocking between the implant biomaterial and the surrounding natural bone can be improved with the porous surface, by providing a greater mechanical stability for this interface [14]. Thus a number of fabrication techniques have been developed to make HA bioceramic, including the

*Corresponding author. Tel.: +86 10 62782770; fax: +86 10 62771160.
E-mail address: biomater@mail.tsinghua.edu.cn (Q. Feng).

0272-8842/$ - see front matter © 2013 Elsevier Ltd and Techna Group S.r.l. All rights reserved.
http://dx.doi.org/10.1016/j.ceramint.2013.04.075

polymer replication method (PRM) [15], solid free form fabrication (SFF) [16], ice templating [17,18] and dual-phase mixing [19]. Many methods such as sintering HA and β-TCP mixture with porogen addition [20], combining gel-casting and freeze drying methods [21] or the polymer template fabrication technique [22] improved the mechanical properties or the corresponding porosity. However, it is difficult to prepare a structure with both higher porosity and higher mechanical properties.

To solve this problem, we tried to obtain a novel structure. Porous HA bioceramics with in-situ grown HA whiskers were prepared using a simple sintering method. The whiskers grew directly from the HA matrix, avoiding the interface problems when physically mixing whiskers with HA matrix. The HA whiskers grew from the cliffs of the pores, almost parallel and stratified. The HA bioceramic has both a high porosity and a high compressive strength, which provides a better environment for cell culture and is more suitable to be used as a bone substitution material. Furthermore, this bioceramic can be molded into any shape so it can easily fill into the complicated fracture. Due to the novel in-situ grown whiskers and the simple manufacturing method, this new kind of porous HA bioceramic with good mechanical properties is attractive in the application as bone substituting material.

2. Materials and methods

2.1. Manufacturing procedure

Polyvinyl alcohol (PVA-124) was first dissolved in heated deionized water under stirring for 24 h until the 5%w/v solution clarified. Then the solution was slowly cooled down to room temperature. 10 g HA powder (Beijing Dk Nanotechnology Co., LTD.) of about 20 nm in diameter was mixed with 3 ml PVA solution using an agate mortar. After prilling, the pre-mixtures were uniform. Hydrated plaster ($CaSO_4 \cdot 2H_2O$) particles were 0.25–0.50 mm in diameter after sieving. The final mixtures were obtained by mixing a certain weight of $CaSO_4 \cdot 2H_2O$ particles with the prepared pre-mixture. The final mixtures consisted of 10 wt%, 20 wt% and 30 wt% $CaSO_4 \cdot 2H_2O$, respectively. All reagents used in the experiments were at analytical grade.

The final mixtures were uniaxially pressed with a force of 150 MPa into cylinders using a 10 mm cylindrical die. The desiccative cylinders were then heated in a furnace (SX-G02163, Tianjin Central Furnace Co., LTD.) with a heating rate of 10 °C/min to 1300 °C. The soaking times were 1 h at 600 °C, and then 2 h at 1300 °C. All samples were cooled in furnace after sintering and kept dry before the following tests.

2.2. Microstructural characterization and mechanical testing

To determine if there was any crystal structural change after sintering, the sintered samples were ground into powder and characterized by X-ray diffraction (D/max 2500 Rigaku X-RAY DIFFRACTOMETER, CuKα, 5°/min, 0.02 per step). The incisions across the samples were observed with SEM after the gold spray treatment. Scanning electron microscopy (SEM; LEO-1530) was used to observe the morphology of the samples. The structure in the samples, including the pores and the whiskers, was analyzed. The length and diameter of the whiskers were also measured on SEM images and the data was based on more than 80 intact whiskers. The specimens were cylindrical of 10 mm in diameter and 10 mm in length after sintering and kept dry before the compression tests. Compression tests were conducted on more than 4 specimens of each series at a crosshead speed of 1 mm/min on the WDW3020 electronic universal experiment machine. The final porosity data of HA bioceramic was calculated automatically with a mercury injection apparatus (Autopore IV 9510). Quantitative data of compressive strength were expressed as the mean ± standard deviation. Statistical analysis was performed using Student's *t*-test or one-way analysis of variance (ANOVA) with software IBM SPSS Statistics 19. A value of $p < 0.05$ was considered to be statistically significant.

3. Results and discussion

3.1. Characterization of the HA bioceramics

The sintered 30 wt% $CaSO_4 \cdot 2H_2O$ sample is shown in Fig. 1. The pores located uniformly in the bioceramic were about 20–200 μm in diameter, caused by the decomposition of $CaSO_4$ into CaO and SO_2 at the temperature above 1220 °C. Some cliffs changed into HA whiskers, as shown in Fig.1b, while some cliffs were substrates for HA whiskers. This porous bioceramic surface can modulate the adsorption of proteins from serum, and the adhesion and proliferation of human bone cells [23]. Furthermore, macro- and micro-porosity in scaffold is better than a uniform pore size for cell culture [24]. So this large range of pore sizes may provide a better environment for the cells. Most whiskers spread in the pores and also some outside the pores, which increased the surface roughness. This rough texture promotes human bone cell attachment [25]. Furthermore, the primary SEM results suggest that the pores are interconnected to a certain extent.

The powder XRD pattern of the 30 wt% sample is presented in Fig. 2. All the peaks, except for some peaks marked with triangle and quadrate, are in agreement with standard hydroxyapatite ($Ca_{10}(PO_4)_6(OH)_2$, JCPDS No.54-0022), indicating that the main phase composition was hydroxyapatite. The two peaks marked with triangles stand for the residual $CaSO_4$ (JCPDS No.37-1496). $CaSO_4$ begins to decompose from above 1220 °C and completely decomposes at 1390 °C [26]. The four peaks marked with quadrates stand for β-tricalcium phosphate (β-TCP) (JCPDS No. 09-0169), which is a product of high temperature decomposition of HA. The XRD powder pattern shows that despite some $CaSO_4$ and β-TCP, the main phase is hydroxyapatite. Considering the morphology of β-TCP and thermodynamically stable HA, the XRD result indicates the whiskers shown in the following SEM micrographs were HA whiskers. HA powders sintered at a high temperature can decompose into β-TCP and tetra-calcium phosphates in dry air while no decomposition of HA occurs

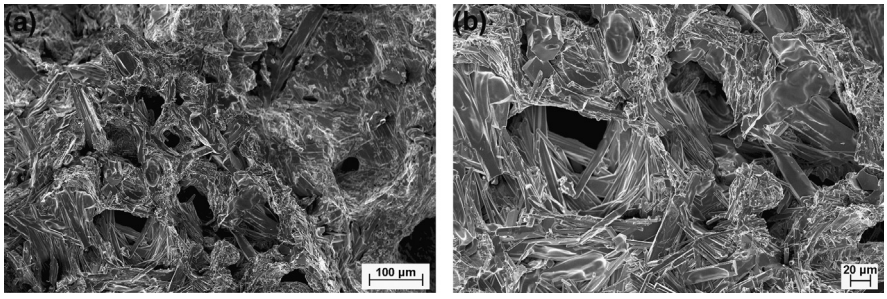

Fig. 1. Sintered 30 wt% $CaSO_4 \cdot 2H_2O$ bioceramics with (a) pores about 100 μm and (b) pores about 40 μm.

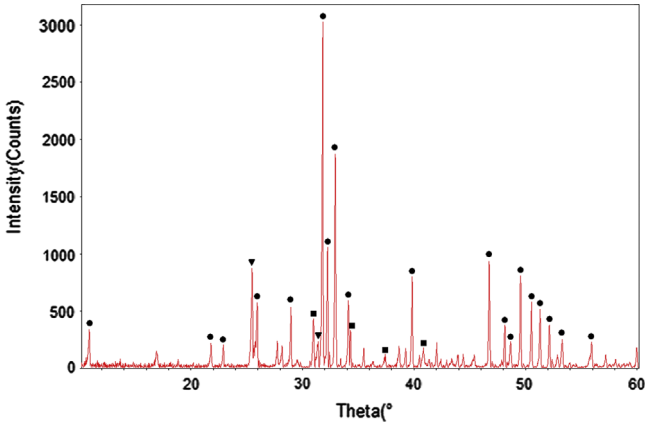

Fig. 2. The powder XRD patterns of sintered 30 wt% $CaSO_4 \cdot 2H_2O$ bioceramic with in-situ grown whiskers.

in moisture [27]. This suggests that the pores might provide a local hydrous environment offered by the bound water of $CaSO_4 \cdot 2H_2O$ while the surface outside the pores was relatively dry. So HA whiskers mainly grew in pores while the decomposition of HA mainly occurred outside the pores.

In Fig. 2, the strongest diffraction peak is (211), and the second strongest peak is (300). However, the (300) peak is stronger than normal. (211) peak of HA is the strongest in general, but the (300) peak becomes the strongest when HA whiskers exist and grow along the *c*-axis [28]. So the stronger (300) peak indicates that the in-situ grown HA whiskers grew along *c*-axis. Furthermore, the spiculate peaks indicated the high HA crystallinity, which was calculated as 91.50%.

Whiskers of different sizes and amounts were observed in all the 10 wt%, 20 wt% and 30 wt% samples. The degree of uniformity in morphology of whiskers was improved and the number of whiskers were increased with the increasing weight of $CaSO_4 \cdot 2H_2O$. The whiskers had a mean length of 48 μm and a mean diameter of 1.3 μm in the 30 wt% sample, as shown in Fig. 3. Most of the whiskers are on the cliffs of pores, some are on the surface. Moreover, whiskers on the cliffs are uniform while whiskers on the surface are disordered and fragmented. This is because the pores provided a specific whisker-growing environment, which is explained in detail below.

The insert EDS result in Fig. 3b shows that the whiskers are composed of calcium and phosphorus, no sulfur is observed. Considering the XRD result, despite some $CaSO_4$ and β-TCP in the sample, these whiskers are all HA whiskers. The small content of Au comes from the gold spray treatment before SEM observation. No grain boundaries are observed on whiskers, suggesting that the whiskers are single crystals. The quantitative EDS results of inner whiskers in Fig. 3b are shown in Table 1. Au comes from the gold spray treatment. The results give a Ca/P ratio of about 2, which indicates that apart from HA and β-TCP, some calcium compound exist. It is most likely CaO, because there is no sulfur detected in EDS and some XRD peaks of CaO may well be superposed with stronger XRD peaks of $CaSO_4$. This indicates that $CaSO_4 \cdot 2H_2O$ decomposes and left CaO in pores during heat treatment, which promotes the nucleation and growth of HA whisker.

The HA whisker bundles grown on cliff are almost parallel to each other, as shown in Fig. 3c. Furthermore, HA whiskers surrounding pores are stratified. Three layers can be seen in Fig. 3c. Each layer is composed of a group of parallel HA whiskers. This may improve the mechanical properties by preventing the cracking of the surface when loaded [29].

At the bottom of the pore, inward tiny HA whiskers were clearly observed, as shown in Fig. 3d. These tiny HA whiskers revealed how the whiskers grew when heated. It can be deduced that the $CaSO_4 \cdot 2H_2O$ loses bound water and provides a local hydrous environment when sintering. Under high pressure caused by residual stress after uniaxial compression, the local hydrous environment provided a hydrothermal condition at the interfaces between $CaSO_4$ and HA nanoparticles. This process lasted for a short time, allowing HA whiskers to nucleate and grow. $CaSO_4$ gradually decomposed into CaO and SO_2 in dry air above the temperature of 1220 °C [23]. This caused $CaSO_4$ particles to turn into smaller CaO powder and make the pore CaO-rich environment. At the grain boundary of HA particle when sintered, nucleation took place and the HA whiskers began to grow during the decomposition of $CaSO_4$. No observation of agglomerate HA whiskers indicates that each whisker grows from its independent nucleation. The morphology of whisker is based on its innate tendency to grow along *c*-axis under certain conditions [30]. However, this is a preliminary result. Further research is necessary to analyze the mechanism of nucleation and growth of the HA whiskers.

3.2. Mechanical testing

Compressive properties and the corresponding porosity of the samples are shown in Fig. 4a. Statistically significant

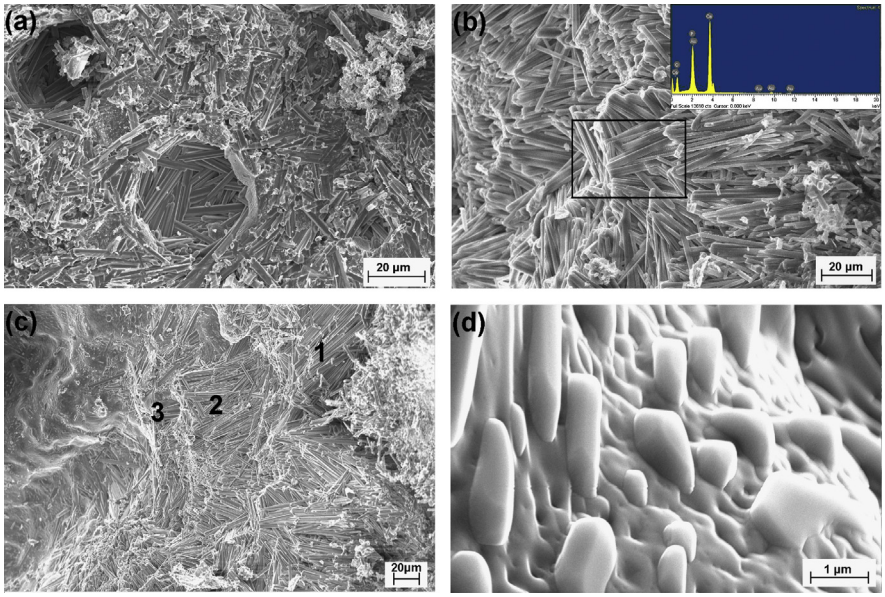

Fig. 3. (a) Small pores in the bioceramic; (b) EDS results of whiskers on the cliff of a pore; (c) the cliff of a pore brimming with 3 whisker layers marked as 1, 2, 3; and (d) tiny crystals on the cliff of a pore.

Table 1
Quantitative EDS results of inner whiskers in 30 wt% $CaSO_4 \cdot 2H_2O$ sample.

Element	Ca	P	O	Au
Atomic%	20.23	10.18	69.19	0.40

difference was observed between the different bioceramic series ($p < 0.05$, $n \geq 3$). According to the compression test data, the compressive strength increased with the weight ratio of 0–20 wt% $CaSO_4 \cdot 2H_2O$ particles. This confirmed the expected results. $CaSO_4 \cdot 2H_2O$ particles contributed to the pores and facilitated the growth of whiskers. Thus more pores and more whiskers were formed as the weight ratio of $CaSO_4 \cdot 2H_2O$ increased. The highest porosity was 42.29%, and the compressive strength was 8.93 ± 0.31 MPa. The highest compressive strength was 21.7 ± 4.4 MPa, with a reduced porosity of 25.97%. The increasing porosity of 0–20 wt% sample depends on the pore-forming of $CaSO_4 \cdot 2H_2O$ particles, but the growth of HA whiskers also occupies the pores and reduces the porosity partly. In our experiment, the main reason of improvement was that despite more pores reducing the compressive strength of the material, more whiskers appeared as an enhanced component. So in 30 wt% sample, the catalytic influence of CaSO4 · 2H2O particles has already exceeded the pore-forming effect. This leads to a more intense increasing of compressive strength and reduction of porosity.

It is reported that the compressive strengths of cervical spine and tibial plateaus are 12.5 ± 0.29 MPa and 13.9 to 23.2 MPa, respectively [31]. Other works found compressive strengths of HA scaffold as 3.56 ± 0.39 MPa with a porosity of 25.7% by PRM and 14.61 ± 1.69 MPa with a porosity of 24.8% by SFF using the tomographic image calculation method [16], or compressive strengths of 10–17 MPa with a porosity of about 24% [21]. HA scaffolds produced by a combination technique [21] and other previous results of porosity and the corresponding compressive strengths are shown in Fig. 4b. Despite the compressive strength of the 30 wt% sample in this work being 21.7 ± 4.4 MPa at porosity of 25.97%, this bioceramic with in-situ grown HA whiskers has a higher compressive strength than previous results in the same range of porosity. The highest compressive strength of HA bioceramic with the porosity of 20–30% in the previous work was 16.5 MPa with a porosity of 23% [21]. Our result gave a compressive strength of 21.7 MPa with a porosity of 25.79%, 31.5% higher in the compressive strength and 12% higher in the porosity. In the higher range of porosity, our result gave a compressive strength of 8.93 MPa, 107.7% higher than a previous work [21] with a slight decrease in porosity (6%). This mainly depends on the novel in-situ grown whiskers in the pores, instead of the pores with relatively smooth cliffs.

An example of compressive curves of three different series is provided in Fig. 5. The two peaks stand for compressive strengths, which are different from common mechanical behavior of brittle materials. It can be defined as a two-step fracture pattern. The two peaks are caused by different fracture factors. It can be deduced that, the first stress, marked with a triangle, was mainly based on the porous matrix and the second fracture, marked with a quadrate, was mainly based on the whisker reinforcement. The compressive strengths of the samples improved with an increased weight ratio of $CaSO_4 \cdot 2H_2O$. Up to 20 wt%, it is different from the former results that higher porosity leads to lower compressive strength. This novel mechanical property is mainly based on the in-situ grown HA whiskers. According to the results of SEM, more $CaSO_4 \cdot 2H_2O$ particles resulted in a more uniform and better morphology and an increasing number of whiskers. The highest compressive strength was observed with the 30 wt% sample. Pores collapsed

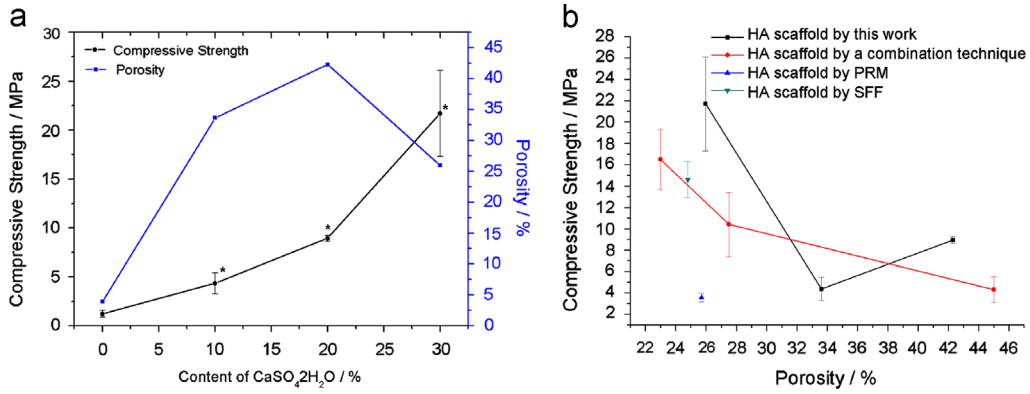

Fig. 4. Compressive strength and porosity of HA bioceramics in (a) this work and (b) comparison between this work and a combination technique [21], PRM [16] or SFF [16], $^{*}p < 0.05$.

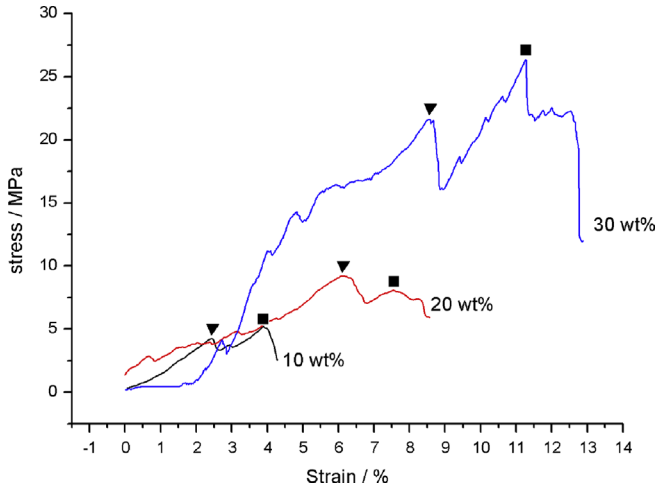

Fig. 5. The example of compression curves of bioceramics containing10 wt%, 20 wt%, 30 wt% $CaSO_4 \cdot 2H_2O$ particles with square marked as the first fracture and triangle as the second.

after the first peak and the whiskers in pores began to play a leading role in mechanical property of the samples. During this period, more whiskers led to a higher compressive strength. Furthermore, 10 wt% samples with shorter and less whiskers showed the similar levels between the first and second fracture stresses, but longer and more whiskers in 30 wt% sample resulted in a much higher second fracture stress than the first. This indicates that the reinforcement of in-situ grown HA whisker is effective, and increasing more radically above 20 wt%. The two-step fracture pattern intimated the mechanism of whisker reinforcement in these samples. Above all, more pores resulted in better environment for cell culture, and higher compressive strength led to a better bone substitution material, both were successfully integrated in one sample.

4. Conclusions

In summary, we prepared a novel porous HA bioceramic with in-situ grown HA whiskers by introducing $CaSO_4 \cdot 2H_2O$ particles, which acted as a pore-forming medium and as a catalyst for the growth of in-situ HA whiskers. Both the compressive strength and the porosity of the HA bioceramic are improved, which provide a new approach to increase the porosity without decreasing the mechanical properties. This is mainly based on its two-step fracture pattern, in which HA matrix and HA whiskers play a leading role respectively. Both the compressive strength and porosity increased in the range of 0–20 wt% samples. HA bioceramic with the compressive strength of 21.7 MPa and a porosity of 25.97% was obtained at the sintering temperature of 1300 °C with 30 wt% $CaSO_4 \cdot 2H_2O$. Similarly, HA bioceramic with the compressive strength of 8.93 MPa and a porosity of 42.29% was obtained at the sintering temperature of 1300 °C with 20 wt% $CaSO_4 \cdot 2H_2O$. The porosity and mechanical properties depend on the structure, which is influenced by the weight ratio of mixed raw materials, pre-compaction and the sintering process. This novel structure provides a promising reinforced pattern for porous materials used as bone substituting material.

Acknowledgments

The authors are grateful for the financial support from the National Natural Science Foundation of China (51072090, 51061130554) and Shenzhen-Hongkong Innovative Circle Project (No: JSE201007200024A).

References

[1] L.L. Hench, Bioceramics—from concept to clinic, Journal of the American Ceramic Society 74 (7) (1991) 1487–1510.
[2] V. Sergey, Dorozhkin, bioceramics of calcium orthophosphates, Biomaterials 31 (7) (2010) 1465–1485.
[3] A. Ito, K. Onuma, Growth of hydroxyapatite crystals, in: T. Ohachi, K. Byrappa (Eds.), Crystal Growth Technology, Springer-Verlag, Berlin, Germany, 2003, pp. 525–548.
[4] W.M. Gao, C.X. Ruan, Y.F. Chen, Effects of hydroxyapatite morphology on the mechanical strength of hydroxyapatite–polyanhydride composites, Journal of Materials Science and Engineering 24 (5) (2006) 646–648.
[5] Z.L. Jin, S.L. Li, W. Li, Performance and applications of whisker-reinforced composite, Journal of the Salt Lake Research 4 (2003) 57–66.
[6] S. Bose, A. Banerjee, S. Dasgupta, A. Bandyopadhyay, Synthesis, processing, mechanical, and biological property characterization of hydroxyapatite whisker-reinforced hydroxyapatite composites, Journal of the American Ceramic Society 92 (2) (2009) 323–330.

[7] B. Rai, L. Grondahl, M. Trau, Combining chemistry and biology to create colloidally stable bionanohydroxyapatite particles: toward load-bearing bone applications, Langmuir 24 (15) (2008) 7744–7749.
[8] G.L. Converse, T.L. Conrad, C.H. Merrill, R.K. Roeder, Hydroxyapatite whisker-reinforced polyetherketoneketone bone ingrowth bioceramics, Acta Biomaterialia 6 (3) (2010) 856–863.
[9] Y. Ota, T. Iwashita, T. Kasuga, Y. Abe, Novel preparation method of hydroxyapatite fibers, Journal of the American Ceramic Society 81 (6) (1998) 1665–1668.
[10] A.C. Tas, Molten salt synthesis of calcium hydroxyapatite whiskers, Journal of the American Ceramic Society 84 (2) (2001) 295–300.
[11] M. Salarian, M. Solati-Hashjin, S.S. Shafiei, A. Goudarzi, R. Salarian, A. Nemati, Surfactant-assisted synthesis and characterization of hydroxyapatite nanorods under hydrothermal conditions, Materials Science — Poland 27 (4) (2009) 961–971.
[12] I.S. Neira, Y.V. Kolen'Ko, O.I. Lebedev, G. Van Tendeloo, H.S. Gupta, F. Guitian, An effective morphology control of hydroxyapatite crystals via hydrothermal synthesis, Crystal Growth and Design 9 (1) (2009) 466–474.
[13] W. Suchanek, M. Yashima, M. Kakihana, M. Yoshimura, Hydroxyapatite/hydroxyapatite-whisker composites without sintering additives: mechanical properties and microstructural evolution, Journal of the American Ceramic Society 80 (11) (1997) 2805–2813.
[14] V. Karageorgiou, D. Kaplan, Porosity of 3D biornaterial bioceramics and osteogenesis, Biomaterials 26 (27) (2005) 5474–5491.
[15] S.W. Yook, H.E. Kim, B.H. Yoon, Y.M. Soon, Y.H. Koh, Improvement of compressive strength of porous hydroxyapatite bioceramics by adding polystyrene to camphene-based slurries, Materials Letters 63 (11) (2009) 955–958.
[16] J. Kim, D. Lim, Y.H. Kim, Y.H. Koh, M.H. Lee, I. Han, A Comparative study of the physical and mechanical properties of porous hydroxyapatite bioceramics fabricated by solid freeform fabrication and polymer replication method, International Journal of Precision Engineering and Manufacturing 12 (4) (2011) 695–701.
[17] Y. Zhang, K.H. Zuo, Y.P. Zeng, Effects of gelatin addition on the microstructure of freeze-cast porous hydroxyapatite ceramics, Ceramics International 35 (2009) 2151–2154.
[18] K. Zhao, Y.F. Tang, Y.S. Qin, J.Q. Wei, Porous hydroxyapatite ceramics by ice templating: freezing characteristics and mechanical properties, Ceramics International 37 (2) (2011) 635–639.
[19] S.H. Li, J.R. De Wijn, P. Layrolle, K. de Groot, Synthesis of macroporous hydroxyapatite bioceramics for bone tissue engineering, Journal of Biomedical Materials Research 61 (1) (2002) 109–120.
[20] A. Bignon, J. Chouteau, J. Chevalier, G. Fantozzi, J.P. Carret, P. Chavassieux, Effect of micro- and macroporosity of bone substitutes on their mechanical properties and cellular response, Journal of Materials Science: Materials in Medicine 14 (12) (2003) 1089–1097.
[21] N. Monmaturapoj, W. Soodsawang, W. Thepsuwan, Porous hydroxyapatite bioceramics produced by the combination of the gel-casting and freeze drying techniques, Journal of Porous Materials 19 (4) (2012) 441–447.
[22] K. Zhao, Y.F. Tang, Y.S. Qin, D.F. Luo, Polymer template fabrication of porous hydroxyapatite bioceramics with interconnected spherical pores, Journal of the European Ceramic Society 31 (1–2) (2011) 225–229.
[23] M. Rouahi, O. Gallet, E. Champion, J. Dentzer, P. Hardouin, K. Anselme, Influence of hydroxyapatite microstructure on human bone cell response, Journal of Biomedical Materials Research A 78A (2) (2006) 222–235.
[24] J.R. Woodard, A.J. Hilldore, S.K. Lan, C.J. Park, A.W. Morgan, J. Eurell, The mechanical properties and osteoconductivity of hydroxyapatite bone bioceramics with multi-scale porosity, Biomaterials 28 (1) (2007) 45–54.
[25] K. Anselme, Osteoblast adhesion on biomaterials, Biomaterials 21 (7) (2000) 667–681.
[26] H.Y. Fan, Mutual Transformation Mechanism of Calcium Sulfate and Calcium Sulfide at High Temperature in Different Reacting Atmosphere, Hangzhou: Zhejiang University, 2004 [dissertation].
[27] P.E. Wang, T.K Chaki, Sintering behavior and mechanical-properties of hydroxyapatite and dicalcium phosphate, Journal of Materials Science: Materials in Medicine 4 (2) (1993) 150–158.
[28] Z.H.Q. Zhang, B.W. Darvell, Synthesis and characterization of hydroxyapatite whiskers by hydrothermal homogeneous precipitation using acetamide, Acta Biomaterialia 6 (8) (2010) 3216–3222.
[29] B.L. Zhou, H.B. Feng, F.T. Zhang, Bionic exploration in composite material, Progress in Natural Science 4 (6) (1994) 713–725.
[30] M. Aizawa, A.E. Porter, S.M. Best, W. Bonfield, Ultrastructural observation of single-crystal apatite fibres, Biomaterials 26 (17) (2005) 3427–3433.
[31] T. Sonoda, Studies on the strength for compression, tension and torsion of the human vertebral column, Jornal of Kyoto Prefectural University of Medicine 71 (1962) 659–702.